

## EFFECT OF COOLING CONDITION ON THE PERFORMANCE OF THERMOELECTRIC POWER GENERATION SYSTEM COUPLING WITH PCM MODULE

by

**Jiapu ZOU<sup>a</sup>, Zihua WU<sup>a</sup>, Anbang LIU<sup>b</sup>, Shi FENG<sup>a</sup>, and Huaqing XIE<sup>a\*</sup>**

<sup>a</sup> School of Energy and Materials, Shanghai Polytechnic University,  
Shanghai, China

<sup>b</sup> School of Energy and Power Engineering, Nanjing University of Science and Technology,  
Nanjing, China

Original scientific paper  
<https://doi.org/10.2298/TSCI200621160Z>

*In this study, a thermoelectric power generation (TEG) system coupling with PCM module for thermal control and storage has been fabricated. Bismuth Telluride ( $\text{Bi}_2\text{Te}_3$ ) TEG devices were applied to convert heat into electricity and Sn-Ag-In alloy PCM was employed for heat storage. A cooling channel with pure water and graphene nanofluids as heat exchange media was attached tightly with the cold-sides of the TEG devices. The effects of the flow rate of cooling water and the mass fraction of graphene nanofluids on the heat transfer process and the performance of the as fabricated TEG-PCM coupling system have been investigated. It is found that increasing the heat exchange capability of the cooling channel would help the PCM module to enhance the heat absorption and utilization of thermal energy from heat source, which in turn brings about the improvement of efficiency of TEG system. The output voltage of TEG system by using pure water for cooling is improved by 6.6%-13.1% with the acceleration of flow rate. Using graphene nanofluids as heat exchange media, the TEG system could achieve 7.2%-18.5% enhancement in output voltage with an increase in the mass fraction of the used nanofluid.*

Key words: TEG, PCM, coupling system, graphene nanofluid

### Introduction

Due to the unreasonable utilization of energy, the shortage of energy has become an essential problem for mankind. Fossil fuels on which the world still depends are finite and far from environmentally friendly. Fossil fuels are mainly burned by internal combustion engines to work or generate electricity. However, not more than 60% heat is used efficiently by internal combustion engines. The engines exhaust would take about 35% of the heat generated by combustion of fuel [1], which causes the inefficient use of energy. Moreover, the emission of engine exhaust could exacerbate the greenhouse effect. Researchers found that a heat source at semiconductor thermoelectric device would cause charge carrier flow away from PN junction, converting heat to electricity [2]. Such technology, called thermoelectric technology, possesses advantages such as ability to utilize low-grade thermal energy, durability and environmental friendliness [3]. The outstanding performance makes thermoelectric technology be

\* Corresponding author, e-mail: hqxie@sspu.edu.cn

applied to various working environments such as micro-generation for micro-electronics [4], waste heat recovery [5, 6], space exploration [7], *etc.*

The efficiency of a TEG device is determined by the performance parameters of thermoelectric material, topology of thermoelectric modules, and temperature difference between the hot and cold sides [8]. The main obstacle to the development of this technology is the relatively low figure of merit,  $ZT$ , of thermoelectric materials. The characteristics of the TEG system itself may affect the power generation capacity of thermoelectric materials. Therefore, optimizing structure and heat transfer capability would be effective ways to improve the performance of a TEG system.

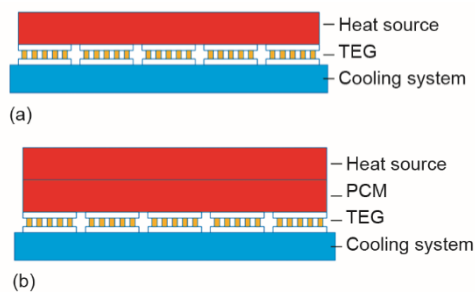


**Figure 1. (a) Construction of a conventional TEG system and (b) a TEG-PCM coupling system**

For the conventional structure of a TEG system presented in fig. 1(a), the heat source directly contacts with the TEG devices. The power output of TEG system would decrease sharply when the heat source stops heat supply, which would cause the low energy utilization rate or even damage the circuit components. Energy harvesting by using heat storage unit (HSU) at the hot side of TEG is a good approach to solve this problem. The PCM which can absorb or release heat by changing from solid to liquid or vice versa are often used as essential components in HSU. The construction of a TEG-PCM coupling system (TEG system coupling with PCM module) is schematically shown in fig. 1(b). Applying PCM module to a TEG system can keep the temperature of its hot side steady and maximize the average temperature difference between the hot- and cold-side of the thermoelectric devices. Fan *et al.* [9] installed paraffin PCM in the middle of thermoelectric devices, and the results showed that the efficiency of TEG after stopping supply of heat. Mao *et al.* [10] investigated the influence of different amount of PCM on thermoelectric generation properties. The results showed that increasing the volume of the PCM could result in an increase in the output voltage. Klein *et al.* [11] presented a design of automotive thermoelectric generators with integrating PCM. The PCM-TEG system was shown to have a higher energy yield than a conventionally constructed TEG system.

On the other hand, enhancing the performance of cooling system at the cold-side of a TEG system can increase the temperature difference between the hot- and cold-sides, and then improve the efficiency of the TEG system. It is expected that, to a thermoelectric power generation system, strengthening the heat transfer capability of the cooling system can result in a remarkable rise in power generation. Nanofluid, as a high performance heat exchange medium, is promising to be employed as the coolant in the cooling system. Li *et al.* [12] experimentally investigated a thermoelectric generation system with minichannel heat exchanger using graphene-water nanofluid as coolant. It is proved that graphene-water nanofluid of 0.1% mass fraction, comparing to pure water, could enhance the output power of the TEG about 114.5%. Nnanna *et al.* [13] experimentally assessed the efficiency of a thermoelectric module with nanofluid heat exchanger. The cooling liquids used are  $Al_2O_3$ -water nanofluid with volume fraction lower than 2% or deionized water. The temperature gradient of nanofluids during the experiment is close to zero, which means the contribution of Fourier effect to the overall heating is approximately zero. Thus, compared to deionized water, heat from the

cold-side of TEG can be absorbed more efficiently. The advantageous influence of nanofluids for cooling the thermoelectric generation system has also been numerically investigated. Haghghi *et al.* [14] showed that the classical correlations developed for pure fluids such as the Shah correlation (for heat transfer) and the Darcy equation (for pressure drop) are valid for the tested nanofluids. Dai *et al.* [15] proposed a general threshold to subdivide a flow in a smooth or a rough micro- and mini-channel in terms of relative roughness. Moraveji *et al.* [16] numerically investigated the effect of nanofluid volume fraction on the convective heat transfer coefficient of minichannel with TiO<sub>2</sub> and SiC nanoparticles. The results showed that the heat transfer coefficient became greater with increasing nanoparticle concentration. However, it is worth noting that the temperature of the cold side decreasing might, in turn, affect the temperature of the hot side and lead to the drop of TEG power output. Jang *et al.* [17] proved this point in their study. The TiO<sub>2</sub>-nanofluid with mass fraction of 0.005% to 0.05% is used as cooling fluid. When the mass fraction is over 0.01%, the temperature difference of TEG is lower than that of 0.005% and 0.05%. It means that increase of mass fraction can enhance heat transfer performance and lead to the temperature decrease of hot side. Therefore, cooling capacity of the working medium has an optimum value.

It has been indicated that the ability of heat harvesting from heat source and capacity of cooling fluid play essential roles in the efficiency of power generation of TEG. Furthermore, the cooling system may have a significant impact on the hot-side of a TEG. However, experimental investigations on the combined influence are still lacking and desirable. In this study, the effect of cooling condition on the performance of TEG-PCM coupling has been experimentally investigated and related heat transfer processes has been explored.

## Experiments

Figure 2 presents the digital images of the experimental system in this study. The main components include TEG-PCM coupling system, cooling liquid circulation system and data acquisition system. The TEG-PCM system is mainly composed of TEG devices, PCM module, and an electric heating plate. These three parts and the cooling liquid channel at the cold-side of TEG devices are fixed by a gripping holder. Heat transfer takes place through cooling liquid channel to cool the TEG system. Figure 3 presents the arrangement of TEG devices on the cooling liquid channel. Ten TEG devices are evenly placed and adhered on the channel using a thermal adhesive with thermal conductivity of 2.0 W/mK (Dow Corning SE4485). All the TEG devices are connected in series into an integrated system by welding and the welded joints are covered by thermal insulation tapes. The  $I_{max}$ ,  $U_{max}$ , and  $Q_{c,max}$  of the TEG are 10 A, 27.4 V, and 148 W, respectively. The positive and negative leads of the TEG

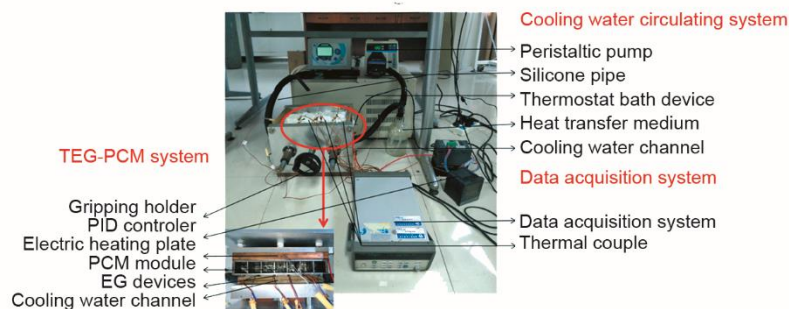
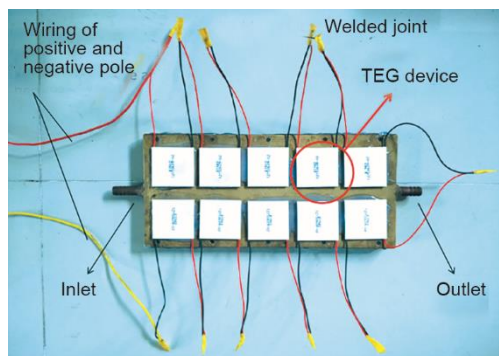


Figure 2. Digital images of the experiment system



**Figure 3.** Arrangement of TEG devices on the cooling liquid channel

a thermoelectric generation system was introduced in our previous study [18].

The cooling circulation system is used to adjust the temperature of the cold-side for the TEG-PCM system. It consists of a cooling channel, thermostat bath, peristaltic pump, heat transfer medium and silicone pipe. The low temperature heat transfer medium is pumped in the cooling channel to cool the TEG devices. After absorbing heat from the TEG devices, the heat transfer medium flow out of the cooling channel, and then flow into thermostat bath device (YB-LS-300W from Shanghai Yi Bei Industrial, temperature control accuracy:  $\pm 0.2$  °C)

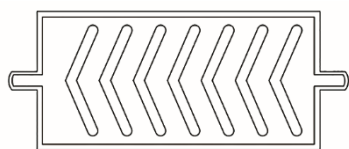


**Figure 4.** Internal structure of cooling channel

to dissipate heat. After heat dissipating, the heat transfer medium subsequently returns to the cooling channel by peristaltic pump and then complete a cycle. The inside diameter of the channel inlet is 7.62 mm. The internal structure of cooling channel is schematically shown in fig. 4. The “A” shaped protuberances in cooling channel can increase the contact area between the heat transfer medium and the wall of channel. It can increase the uniform distribution of temperature and thus improve the efficiency of TEG devices [19]. The heat transfer media used in this study are pure water and graphene nanofluids composed of a base fluid (50% glycol solution and 50% purified water) and different mass fractions (0%, 0.1%, and 0.2%) of graphene oxide nanosheets (GNS), respectively. The preparation of GNS nanofluid has been described in [20]. Silicone pipe is used for connecting the components of the cooling system because it is suitable for carrying nanofluids due to its great wear and corrosion resistance.

The data acquisition system is used to collect the signals of the output voltage of TEG device and the temperatures of PCM module and fluid at the inlet and outlet of the cooling channel. This system is composed of a PC, data acquisition device and thermocouples embedded in the components of TEG-PCM system. The measured output voltage of TEG devices is open-loop voltage and tested by a voltage device (America Agilent Technologies Joint Stock Company, version 34970A, measurement accuracy:  $\pm 1\%$ ). The temperatures of heat transfer medium in the inlet and outlet of cooling channel are tested by thermocouples embedded inside the inlet and outlet pipe. And the temperature of PCM module is tested by a thermocouple embedded at the center of the PCM. All the temperature signals are processed using the temperature module in the data acquisition device. The thermocouples used in the

system are connecting to the data acquisition device. At the hot-side of the TEG system, the output of electric heating plate was controlled by a proportional integral derivative (PID) controller (Teshow EM405). The PCM module absorbs the heat from the electric heating plate and then provides heat for thermoelectric modules. The composition of the PCM is Sn-Ag-In alloy with a density of  $7.25 \text{ g/cm}^3$  and melting point in the range of 192-198 °C. The phase change latent heat of the used PCM is 58 J/g. When the electric heating plate stops working, the PCM can provide heat for TEG continuously. The detailed function of analogous PCM in

experiments are *K*-type (KMTXL-040G-6 from America OMEGA Engineering Joint Stock Company, measurement accuracy:  $\pm 1.1$  °C).

During the experiments, the temperature of heat plate was set to 300 °C by the PID controller, and the cooling water temperature was stabilized at 30 °C by the thermostat bath. The cooling fluid flow rate was changed by adjusting the rotation rate of peristaltic pump. The rpm of peristaltic pump was set at 100, 200, and 300 rpm, which means 100, 200, and 300 mL per minute of cooling fluid flows through the cooling channel, respectively.

## Results and discussions

### *Effect of the flow rate of cooling water*

The heat transfer process at the cold-side of the TEG devices would affect the overall heat transfer behavior in the TEG-PCM system as well as the cold-side temperature substantially. It is expected that adjusting the heat transfer conditions can be used to change the performance of TEG-PCM system. In order to explore the affecting parameters, firstly pure water was used as heat exchange medium and the flow rate was set at different values. Figure 5 presents the variation in temperature of PCM over the change of the flow rate of cooling water. The temperature change undergoes following processes. When heating, the PCM absorbs heat from the electric heating plate, resulting in the temperature of PCM increases from initial time to about 5000 seconds. We define this period as temperature-rise period (Period 1). In this period, solid-liquid phase change takes place in the PCM and the trend of temperature rise is slow down from about 2500 seconds to about 4000 seconds. The PCM completely melted at about 4000 seconds, thermal convection of PCM in liquid phase further enhances the heat transfer from electric heating plate to the PCM. Thus, the temperature of PCM rises even more quickly from about 4000 seconds to about 5000 seconds compared to that in the time range of initial stage to about 2500 seconds in which heat transfer process is conduction in solid state. At about 5000 seconds, the heat loss and heat absorption in PCM module are balanced and the temperature of PCM reaches its stable value. In order to ensure the stabiliza-

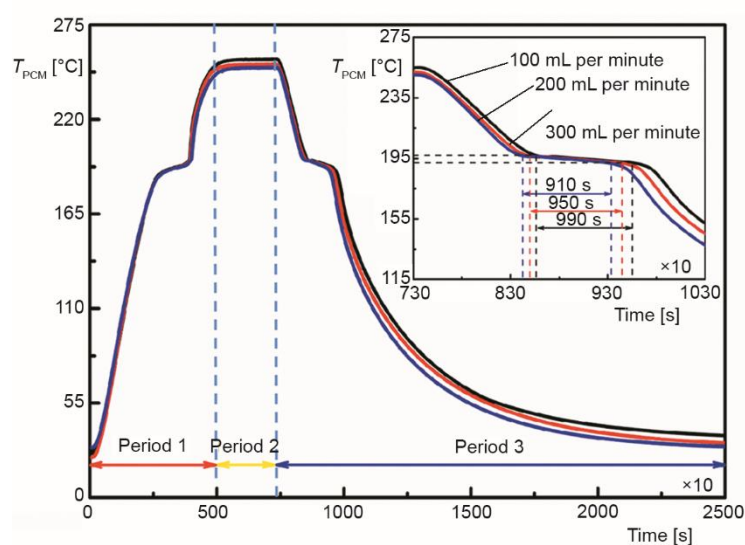


**Figure 5.** Temperature variation of the PCM under different flow rate of cooling water

tion of temperature and the accuracy of experimental data, the heating is maintained to about 7300 seconds. The PCM undergoes a constant temperature period (Period 2) from about 5000 seconds to 7300 seconds. Then the heating stopped and the PCM continues to release heat and plays the role of heat source for that TEG system after 7300 seconds. We define this period as temperature fall period (Period 3). From 7300 seconds to about 8400 seconds, due to the reduction of thermal convection coefficient caused by the decrease of temperature, the temperature drop rate is smaller than the temperature increase rate from about 4000 seconds to 5000 seconds. From 8400 seconds to 9700 seconds, the temperature decrease rate becomes small because of liquid-solid phase change in PCM. As the temperature difference between both sides of PCM module gradually decreases, heat conduction from PCM module to TEG module is reduced. Accordingly, the decline of PCM temperature gradually slows down after about 9700 seconds.

During the Period 1 presented in fig. 5, the trends and values of temperature under different condition of flow rate are almost the same. The PCM subsequently reaches the highest temperature in Period 2. There are slight decreases (no more than 5 °C) among the temperature values of PCM with increase flow rate of cooling water. It is worth noting that, during the Period 3, the process of phase transition of PCM obviously changes. When accelerating the flow rate of cooling water, the starting has been shift to an earlier time. It is observed that the starting time under conditions of 200 mL per minute and 300 mL per minute is about 80 seconds and 60 seconds earlier than that of 100 mL per minute. But the duration time of liquid-solid phase change process is about 40 seconds and 80 seconds shorter than that of 100 mL per minute. It indicates that the flow rate of cooling water can affect the phase transition process of PCM significantly. The increase of flow rate can improve the convective heat

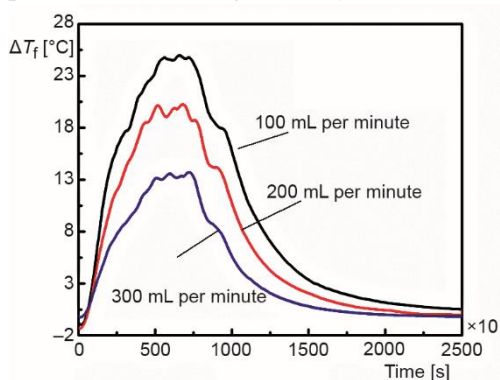


**Figure 6. Temperature differences between outlet and inlet of coolant under different flow rates**

transfer capacity of cooling water to bring away heat from PCM more quickly. Accordingly, the acceleration of cooling water flow rate leads to the advance of phase change process and shortening its duration. It causes temperature change of hot-side of TEG module and subsequently affects the output of TEG devices.

The temperature differences between outlet and inlet of coolant,  $\Delta T_f$ , under different flow rates is shown in fig. 6. The temperature trend are similar to that of PCM shown in fig. 5. It indicates the influence of cooling water on the heat transfer in TEG-PCM coupling system. There are evident differences in temperature differences of cooling water under different conditions. As shown in fig. 6, the  $\Delta T_f$  is decreased with the accelerating of flow rate. The maximum  $\Delta T_f$  under flow rates of 200 mL per minute and 300 mL per minute are nearly 4.9 °C and 11.4 °C lower than that of the 100 mL per minute, respectively. Due to the increase of flow rate, there is more heat transfer medium flow through cooling channel per unit time, resulting in higher heat carrying capacity of cooling water. It causes the temperature of cooling fluid shows downtrends when accelerating flow rate. The heat taken by the cooling water from the cold-side of TEG,  $Q_c$ , can be calculated by the following expression:

transfer capacity of cooling water to bring away heat from PCM more quickly. Accordingly, the acceleration of cooling water flow rate leads to the advance of phase change process and shortening its duration. It causes temperature change of hot-side of TEG module and subsequently affects the output of TEG devices.

The temperature differences between outlet and inlet of coolant,  $\Delta T_f$ , under different flow rates is shown in fig. 6. The temperature trend are similar to that of PCM shown in fig. 5. It indicates the influence of cooling water on the heat transfer in TEG-PCM coupling system. There are evident differences in temperature differences of cooling water under different conditions. As shown in fig. 6, the  $\Delta T_f$  is decreased with the accelerating of flow rate. The maximum  $\Delta T_f$  under flow rates of 200 mL per minute and 300 mL per minute are nearly 4.9 °C and 11.4 °C lower than that of the 100 mL per minute, respectively. Due to the increase of flow rate, there is more heat transfer medium flow through cooling channel per unit time, resulting in higher heat carrying capacity of cooling water. It causes the temperature of cooling fluid shows downtrends when accelerating flow rate. The heat taken by the cooling water from the cold-side of TEG,  $Q_c$ , can be calculated by the following expression:

$$Q = m_v c_p \rho \Delta T_f \quad (1)$$

where  $m_v$  is the volume flow rate of fluid through the cooling channel and  $c_p$  – the specific heat capacity of fluid. The heat exchange rate between TEG and cooling channel under different flow rate conditions of 100, 200, and 300 mL per minute are about 172.9, 269.5, and 273.0 W, respectively. Because the PCM stores approximately the same amount of heat after heating, cooling water with higher flow rate can take away more heat from TEG thereby lower the cold side temperature of TEG devices.

Figure 7(a) presents the output voltage of TEG module,  $U_{out}$ , after Period 1 under different cooling water flow rates. It can be clearly seen that the TEG with higher flow rate of cooling water in the channel at the cold-side can obtain larger output voltage in the test time range. The maximum  $U_{out}$  of TEG system under the flow rates of 300 and 200 mL per minute are 3.2 V and 1.6 V larger than that of 100 mL per minute, which are increases of 13.1% and 6.6%, respectively. Due to the Seebeck effect, the temperature difference between hot- and cold-sides of the TEG device affects the output voltage directly. The temperature of hot-side of TEG device depends on the amount of heat transfer from PCM module. From fig. 5, it is observed that the temperature value and drop rate of PCM before the end of the process of liquid-solid phase change are very close. It is reasonable to consider that the heat transfer rates between PCM module and TEG devices are almost the same during this time range. Thus, there are no much difference in temperatures of hot-side of TEG under different conditions, and the temperature difference between hot- and cold-sides of the TEG mainly depends on the cold-side of TEG. From fig. 6, TEG under higher cooling water flow rate get lower temperature at the cold-side of TEG, resulting in an increase in the temperature difference between hot- and cold-sides of the TEG. Accordingly, TEG under higher cooling water flow rate of can obtain higher  $U_{out}$  before the end of liquid-solid phase change process of PCM. Furthermore, the temperature of PCM reduces faster with higher flow rate after phase change. There is little difference among the cooling water under different conditions in this time range. As a result, the  $U_{out}$  of TEG reduces more quickly with higher flow rate after phase change process.

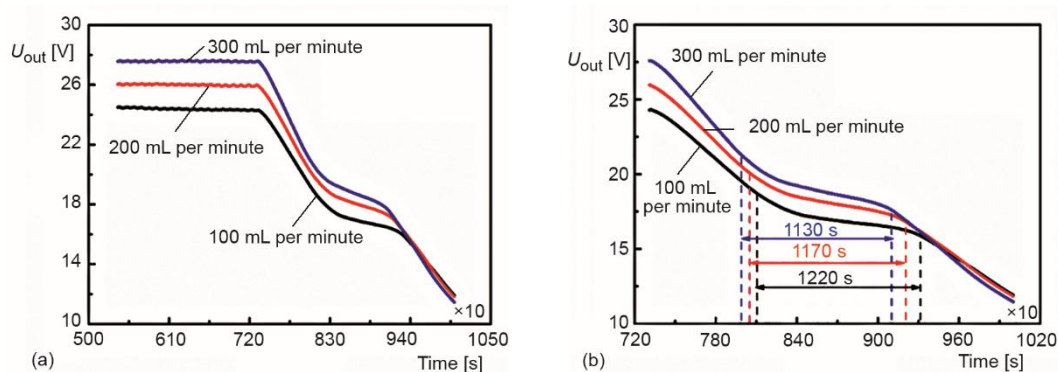


**Figure 7. Output voltage of TEG under different flow rates after temperature-rise period (a) and after heating (b)**

Figure 7(b) shows the output voltages of TEG after heating was stop at 7300 seconds. During this period, PCM acts as the heat source for the TEG devices. Due to the phase

change of PCM, the decrease of  $U_{\text{out}}$  slows down at about 8000 seconds, and the output voltages are in relatively stable state in this time range. The drop rate of output voltage under different conditions speeds up at different times, as shown in fig. 7(b). This speeding-up moment under flow rate conditions of 300 and 200 mL per minute are 180 seconds and 95 seconds earlier than that of 100 mL per minute, respectively. This change is similar to the temperature change of PCM as shown in fig. 5. It indicates that temperature change caused by PCM phase change process would directly affect the  $U_{\text{out}}$  of TEG. To sum up, for TEG-PCM system, increasing the flow rate of cooling water can increase the temperature difference of TEG devices and then improve the output voltage before the liquid-solid phase change process of PCM. On the other hand, when accelerating the flow rate of cooling water, the time for  $U_{\text{out}}$  in relatively steady state will be reduced and the voltage will drop faster after the process of phase change.

#### *Effect of the mass fraction of nanofluid for cooling*

In addition to the flow rate, the heat transfer capacity of the heat exchange medium is also an important factor affecting the cold-side temperature of TEG devices. It is proved that the increase of mass fraction can affect the heat transfer capability of nanofluids [21-23]. In order to investigate this effect, graphene nanofluids with different mass fraction were used as heat exchange media and the flow rate was set at 300 mL per minute. Figure 8 presents the temperature of PCM of the coupling system with different graphene nanofluids as heat transfer medium in cooling channel. It is observed that the variation trend of the temperature is similar to that shown in fig. 5. In the Period 2, the highest temperature of PCM under the cooling conditions with graphene nanofluids of mass fraction of 0.1% and 0.2% are about 2.5 °C and 5.2 °C lower than that of base fluid, respectively. The liquid-solid phase change process under the cooling conditions with 0.1% mass fraction of graphene nanofluids is 50 seconds earlier and 20 seconds shorter than that of base fluid. But starting time of this process when using 0.2% mass fraction of nanofluid is about 160 seconds earlier than that of base fluid, while the time of phase change process is nearly 50 seconds shorter. Accordingly, increasing the mass fraction of nanofluids for cooling has similar effect as increasing the flow rate of fluids.

The variation in temperature difference of heat transfer medium between inlet and outlet of cooling channel with different mass fractions of graphene nanofluids as working medium is depicted in fig. 9. The trend of temperature in fig. 9 is similar to that in fig. 6. The increase in mass fraction of nanofluid and flow rate have similar impact on the temperature difference of fluid. As shown in fig. 9, during the temperature constant period, the average of temperature difference between outlet and inlet under the cooling conditions with graphene nanofluids of mass fraction of 0.1%, and 0.2% are 1.2 °C, 4.4 °C higher than that of base fluid, respectively. It is indicated that the cooling rate has been improved with the increase in the mass fraction.

Figure 10(a) shows the output voltage of TEG system when the as fabricated PCM-TEG coupling system was conducted using graphene nanofluids with different mass fraction as heat transfer media after Period 1. The varying trend of  $U_{\text{out}}$  is similar to that in fig. 7(a). It can be seen that  $U_{\text{out}}$  increases with the mass fraction of the nanofluid used. Compared to the base fluid, graphene nanofluids with mass fractions of 0.2% and 0.1% can help to enhance the maximum  $U_{\text{out}}$  of TEG system 3.6 V and 1.4 V, which are increases of 18.5% and 7.2%, respectively. In this study, the improvement of  $U_{\text{out}}$  of TEG can be attributed to the in-

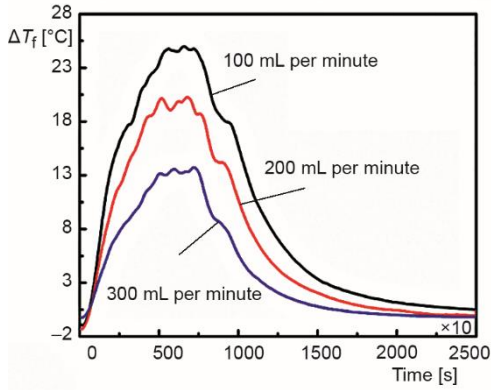


**Figure 8.** Temperature of PCM with nanofluid as heat transfer medium in cooling channel

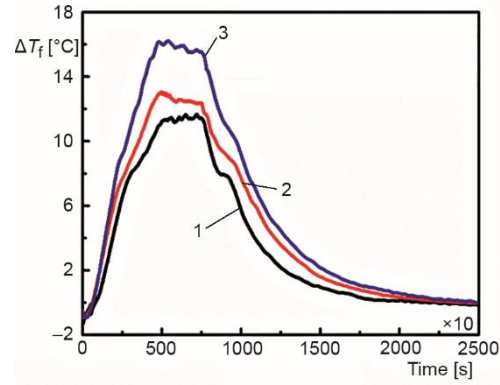


**Figure 9.** Temperature difference between outlet and inlet of cooling channel with different mass fraction of nanofluid as working medium; 1 – base fluid + graphene (0%), 2 – base fluid + graphene (0.1%), 3 – base fluid + graphene (0.2%)

crease in temperature difference between both sides of the TEG. Considering the temperature difference between inlet and outlet of cooling channel under different conditions presented in fig. 9, it can be concluded that the heat flow through TEG devices is improved. The heat flow through TEG,  $q$ , can be expressed by:

$$q = \frac{T_h - T_c}{R} \quad (2)$$

where  $T_h$  and  $T_c$  are the temperature of the hot- and cold-sides of TEG and  $R$  - the thermal resistance between both sides of TEG. Because the output voltage tested is open-loop voltage, and thereby the current in TEG is very low, which has little influence on thermal resistance. So, in this experiment,  $R$  under different conditions can be considered in equal. Thus, from eq. (2), it can be inferred that the difference of  $T_h$  and  $T_c$  is increased. As a result, the output of TEG is improved because of Seebeck effect.

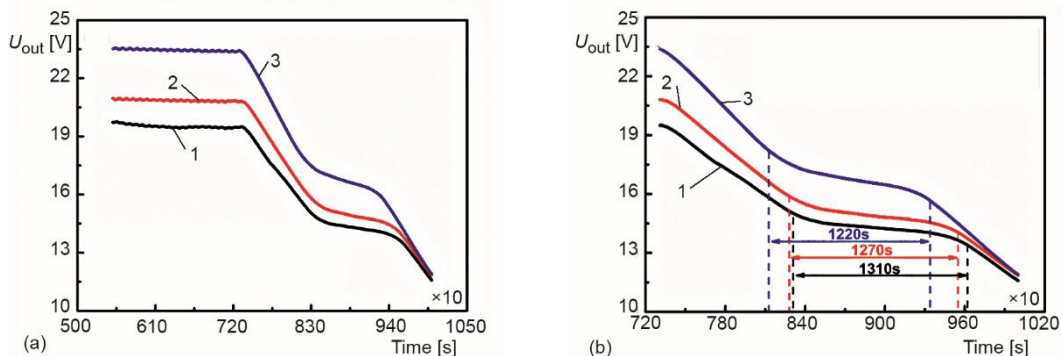


**Figure 10.** Output voltage of TEG using graphene nanofluids with different mass fraction as heat transfer medium after temperature-rise period (a) and after heating stopped (b); 1 – base fluid + graphene (0%), 2 – base fluid + graphene (0.1%), 3 – base fluid + graphene (0.2%)

Figure 10(b) illustrates the times of the output voltage in relatively stable stage under different cooling condition after heating. For the cooling conditions using graphene nanofluid with a mass fraction of 0.2%, the drop of voltage slows down at about 8120 seconds, which is about 190 seconds earlier than that of using base fluid. The time duration in which  $U_{out}$  remains relatively stable is nearly 1220 seconds, which is 90 seconds shorter than that of using base fluid. Because the heat transfer performance of 0.1% mass fraction of nanofluid is not significantly improved compared with that of the base fluid. The starting time and length of the relatively stable period of voltage are just 30 seconds earlier and 40 seconds shorter than that of using base fluid. When heating stopped, the temperature of PCM will directly affect the heat flow through the TEG after heating, and then change the trend of the voltage. Therefore, the  $U_{out}$  show similar trend with  $T_{PCM}$ .

### Conclusion

The effects of cooling capacity at the cold-side of a TEG system on the heat transfer processes and output voltage of have been experimentally investigated. The TEG system was integrated with a PCM module at the hot-side for thermal control and storage. The cold-side of this TEG-PCM coupling system was attached tightly with cooling channel using pure water and graphene nanofluids as heat exchange media. For pure water as heat exchange medium, increasing the flow rate helps to enlarge the temperature difference between the hot- and cold-sides of the TEG devices, resulting in the enlargement of output voltage. The increase of the flow rate of cooling water from 100 mL per minute to 200 mL per minute and then to 300 mL per minute led to the enhancement ratios of the maximum output voltage about 6.6% and 13.1%, respectively. For graphene nanofluids as heat exchange media, increasing the mass fraction of nanofluids has remarkable effects on improving the performance of the as-fabricated TEG-PCM system. When using nanofluids with 0.1% and 0.2% mass fraction graphene dispersed, the enhancement ratios of the maximum output voltage of about 7.2% and 18.5% have been achieved. It is clarified that the two ways employed in this study to enhance the heat transfer capacity of cooling channel have similar influences on the phase change process of PCM module then enlarge the output voltage of the TEG-PCM coupling system.

### Acknowledgment

This work was supported by the National Natural Science Foundation of China (51676117), *Shu Guang* project of Shanghai Municipal Education Commission and Shanghai Education Development Foundation (18SG54), and Shanghai Polytechnic University Graduate Program Foundation (EGD18YJ0018).

### References

- [1] Rowe, D. M., et al., Weight Penalty Incurred in Thermoelectric Recovery of Automobile Exhaust Heat, *Journal of Electronic Materials*, 40 (2011), 5, 784
- [2] DiSalvo, F. J., Thermoelectric Cooling and Power Generation, *Science*, 285 (1999), 5428, 703
- [3] Al-Nimr, M. A., et al., Modeling and Simulation of Thermoelectric Device Working as a Heat Pump and an Electric Generator under Mediterranean Climate, *Energy*, 90 (2015), Oct., pp. 1239-1250
- [4] Shi, Y., et al., A Novel Self-Powered Wireless Temperature Sensor Based on Thermoelectric Generators, *Energy Conversion and Management*, 80 (2014), Apr., pp. 110-116
- [5] Bell, L. E., Cooling, Heating, Generating Power, and Recovering Waste Heat with Thermoelectric Systems, *Science*, 321 (2008), 5895, 1457
- [6] Karri, M., et al. Thermoelectrical Energy Recovery from the Exhaust of a Light Truck, *Proceedings*, 9<sup>th</sup> Diesel Engine Emissions Reduction (DEER) Workshop 2003, Newport, R. I., USA, 2003

- [7] El-Genk, M. S., et al., Efficient Segmented Thermoelectric Unicouples for Space Power Applications, *Energy Conversion and Management*, 44 (2003), 11, pp. 1755-1772
- [8] Deng, Y. D., et al., Modular Analysis of Automobile Exhaust Thermoelectric Power Generation System, *Journal of Electronic Materials*, 44 (2015), 6, pp. 1491-1497
- [9] Fan, W. Y., et al., A smart PV Cooler Based on Solar Thermoelectric Generator with Phase Change Material, *Advanced Materials Research*, 986-987 (2014), July, pp. 1163-1168
- [10] Mao, J. H., et al., Power Generation by Thermoelectric Generator Using Different Amounts of Phase Change Materials, *Journal of Thermophysics and Heat Transfer*, 32 (2018), 3, pp. 799-805
- [11] Klein, A. M., et al., Integrating Phase-Change Materials into Automotive Thermoelectric Generators, *Journal of Electronic Materials*, 43 (2014), 6, pp. 2134-2140
- [12] Li, Y. H., et al., Study on the Performance of TEG with Heat Transfer Enhancement Using Graphene-Water Nanofluid for a TEG Cooling System, *Science China Technological Sciences*, 60 (2017), 8, pp. 1168-1174
- [13] Nnanna, A. G. A., et al., Assessment of Thermoelectric Module with Nanofluid Heat Exchanger, *Applied Thermal Engineering*, 29 (2009), 2, pp. 491-500
- [14] Haghghi, E. B., et al., Cooling Performance of Nanofluids in a Small Diameter Tube, *Experimental Thermal and Fluid Science*, 49 (2013), Sept., pp. 114-122
- [15] Dai, B., et al., Effect of Surface Roughness on Liquid Friction and Transition Characteristics in Micro- and Mini-Channels, *Applied Thermal Engineering*, 67 (2014), 1, pp. 283-293
- [16] Moraveji, M. K., et al., CFD Investigation of Nanofluid Effects (Cooling Performance and Pressure Drop) in Mini-Channel Heat Sink, *International Communications in Heat and Mass Transfer*, 40 (2013), Jan., pp. 58-66
- [17] Jang, J., et al., Thermoelectric Power Generation System with Loop Thermosyphon and TiO<sub>2</sub>-Nanofluids, *Advanced Materials Research*, 535-537 (2012), June, pp. 2100-2103
- [18] Liu, A., et al., Improving the Performance of TEM Embedded with Paraffin-Based Phase Change Materials with Different Thermal Conductivity, *Journal of Renewable and Sustainable Energy*, 11 (2019), 5, 054701
- [19] Liu, X., et al., Experiments and Simulations on Heat Exchangers in Thermoelectric Generator for Automotive Application, *Applied Thermal Engineering*, 71 (2014), 1, pp. 364-370
- [20] Li, Y., et al., The Preparation, Characterization and Application of Glycol Aqueous Base Graphene Oxide Nanofluid, MATEC Web Conference, 238 (2018), 02001
- [21] Li, Z., et al., Experimental Study of Temperature and Mass Fraction Effects on Thermal Conductivity and Dynamic Viscosity of SiO<sub>2</sub>-Oleic Acid/Liquid Paraffin Nanofluid, *International Communications in Heat and Mass Transfer*, 110 (2020), Jan., 104436
- [22] Askounis, A., et al., Effect of Particle Geometry on Triple Line Motion of Nano-Fluid Drops and Deposit Nano-Structuring, *Advances in Colloid and Interface Science*, 222 (2015), Aug., pp. 44-57
- [23] Sedeh, R. N., et al., Experimental Investigation toward Obtaining Nanoparticles' Surficial Interaction with Basefluid Components Based on Measuring Thermal Conductivity of Nanofluids, *International Communications in Heat and Mass Transfer*, 103 (2019), Apr., pp. 72-82